J. Membrane Biol. 96, 251–262 (1987)

The Journal of
Membrane Biology

Evidence for Multiple Open States of Sodium Channels in Neuroblastoma Cells

Károly Nagy
I. Physiologisches Institut der Universität des Saarlandes, D-6650 Homburg/Saar, Federal Republic of Germany

Summary. Open times of voltage-gated sodium channels in neuroblastoma cells were measured during repolarization (following a short depolarizing conditioning pulse) and during moderate depolarization. Conditional and unconditional channel open-time histograms were best fitted by the sum of two exponentials. (The conditional open time was measured from the end of the conditioning pulse until an open channel shuts provided it was open at $t = 0$). Time constants of both histograms depended on the postpulse and were shifted to more positive potentials with increasing conditioning pulse potential. This shift could be explained by assuming more than two time constants in the histograms, which could not be separated. Channel open-time histograms from single-pulse experiments showed a maximum at $t > 0$. These histograms could be best fitted by an exponential function with three time constants. One term of this function included the difference of two exponentials resulting in a maximum at $t > 0$. Open-time histograms showed a definite time dependence. At 2 to 6.5 msec after the beginning of the depolarization the best fit could be obtained by the difference of two exponentials. To these components another term had to be added at 0 to 2 msec. Between 6.5 and 14.0 msec the sum of two exponentials, and after 14.0 msec a single exponential resulted in a good fit. The results support the hypothesis that sodium channels in neuroblastoma cells may have multiple open states. Two of these states are irreversibly coupled.

Key Words neuroblastoma cells · single sodium channels · open-time histogram · multiple open states

Introduction

Kinetic models which describe the function of the voltage-gated sodium channels in excitable cells are developed with the following general assumptions: a) The channels must have a homogeneous population. b) The kinetic parameters are a function of the membrane potential, but not the time. c) The conductance and open-close kinetics of a channel are independent from the other channels (for a review *see* French & Horn, 1983). In several preparations, however, one or more of these assumptions turned out to be violated (*see also* French & Horn, 1983). It was reported that two populations of sodium channels exist in heart cells (Cachelin et al., 1983; Kunze et al., 1985), in myoblasts and myotubes (Weiss & Horn, 1986), in dorsal root ganglion neurons (Kostyuk et al., 1981) and in squid axon (Gilly & Armstrong, 1984). In muscle cells the gating properties of Na channels are changed in time (Patlak & Ortiz, 1986; Patlak et al., 1986). Indications for changes in the unitary conductance and gating properties of channels, probably induced by the interaction of channels, have also been reported (Neumcke & Stämpfli, 1983; Kiss & Nagy, 1985).

Most of the models of sodium channels include several closed states, but generally only one open state. In some preparations, however, the presence of two (or more) open states of channels have been proposed (Frankenhaeuser & Hodgkin, 1957; Chandler & Meves, 1970; Armstrong & Bezanilla, 1977; Armstrong & Gilly, 1979; Sigworth, 1981). It was reported (Nagy et al., 1983) that sodium channels in neuroblastoma cells may also have multiple open states. Recently, the observation of multiple discrete current levels of an open channel provided evidence for the multiple open conformations of these channels (Nagy & Bagany, 1986; Nagy, 1987).

Further properties of sodium channels are described in the present paper. Open times of channels measured during repolarization and depolarization have been analyzed and compared. Results show a complex kinetic behavior of open channels. The time constants of the open-time histograms changed with the initial condition and with time suggesting the presence of several open states. Two open states are sequentially coupled in the early phase of depolarization.

Materials and Methods

Single sodium channel currents were measured in cultured mouse neuroblastoma cells, N1E 115. Cells were grown under

standard conditions as described by Moolenaar and Spector (1978). The experimental methods have been published (Nagy et al., 1983) and will be summarized briefly.

Single-channel current records were obtained using cell-attached patch configuration (Hamill et al., 1981). Lipid-coated pipettes regularly formed a typical seal with a resistance of 40 to 60 Gohm. The membrane was hyperpolarized by 40 to 80 mV to remove resting inactivation. From this constant holding potential depolarizing pulses were applied with 1/sec repetition.

In single-pulse experiments 20- to 40-msec-long pulses to potential of ±10 mV around the cell's resting potential were used. The aim of these experiments was to study the time dependence of the channel open time. Therefore, stronger depolarizations, which shift the channel openings to the beginning of the depolarization, could not be used.

To measure single-channel currents during repolarization a 2-msec-long prepulse was followed (without gap) by 16-msec-long postpulses of different heights. Prepulse potentials were 10 to 40 mV more positive than the cell's resting potential. The mean resting potential of the cells was around −40 mV (*see* Nagy et al., 1983).

Due to the uncertainty of the cell's resting potential parameters of different patches cannot be pooled or compared directly. Instead, long experiments with single patches were used for the present analyses. In Fig. 3(*d*), where parameters of different patches are plotted on a common voltage axis the time constants of the first latency density functions were used to compare and to recalculate the pulse potentials. For this reason, to obtain the unconditional first latency densities in double-pulse experiments, single pulses with two to four different potentials were also applied in every patch.

Pipette and bath solutions contained (in mM): NaCl 140, KCl 5.0, $CaCl_2$ 1.8, $MgCl_2$ 0.8, HEPES 20, glucose 20. pH was adjusted to 7.3 and temperature (between 8 and 15°C) was kept constant during each experiment.

Details of the measuring system are described by Hof (1986) and are summarized briefly as follows. A DEC LSI 11/23 microcomputer generated the voltage pulses, collected the data with 10 kHz sampling rate and was used for off-line analyses. Analog signals were filtered at 2 kHz (−3 dB) by a four-pole low-pass Bessel filter. Leakage and capacitive currents were compensated by an analog circuit.

Data Analysis

Calculations and calibrations have been made to determine the kinetic parameters of the recording system. The parameters were estimated by using the equations of Colquhoun and Sigworth (1983). With a filter frequency of 2 kHz (−3 dB) these calculations result in the following values: 0.166 msec for the rise time and 0.090 msec for the dead time. The signal-to-noise ratio was >8.33. The measured dead time was 0.093 msec, which is very close to the calculated value.

The half-amplitude threshold detection was used for calculations of the open, conditional open and delay times of channel openings, with the accuracy of the sampling interval of 0.1 msec. Note that the expression "conditional open time (COT)" is used in this paper for the time measured from the onset of the postpulse until a channel shuts provided it was open at the end of the conditional prepulse; *see* Fig. 1.

Histograms were constructed with a binwidth of 0.1 msec from at least 200 current records measured with a certain pre- and postpulse. The dead time of the recording and analyzing system (0.093 msec) is very close to the sampling interval. Therefore, the first bin of the open-time histograms (which contains events having open times <0.1 msec) is strongly biased, and so omitted. If histograms are constructed from events having durations greater than twice the dead time, the time constants can be estimated with only a few percent of error. In this case, the number of states can be estimated from the number of exponential components (*see* Roux & Sauvé, 1985; Blatz & Magleby, 1986). Digitization may cause an error in the weight (but not in the time constant) of an exponential component, if the time constant approaches the sample interval (Sine & Steinbach, 1986). Because no conclusions were drawn from the weighting factors corrections for this distortion have not been made.

Capacitive currents often changed during the course of a long experiment. Although careful compensations have been made, occasionally a current peak appeared. The peak at the onset of the postpulse (which could have falsified the conditional open-time measurement) never lasted longer than 0.3 msec. Therefore, conditional open-time histograms were constructed from conditional open-times longer than 0.4 msec.

Patches contained more than one channel resulting in overlapping openings at the onset of the postpulse (*see* Fig. 1). Measuring the time to the first shut the obtained time constant of the conditional open-time histogram should be corrected for the channel number like a first latency density (*see* Patlak & Horn, 1982; Aldrich et al., 1983). The error in the estimation of the channel number, however, can be large. Therefore, all consecutive closings (until an opening occurred) to a maximum of four superimposed openings were measured at the multiples of the half-amplitude threshold (i.e. at 7, 5, 3 and 1× the threshold). In this way, patches with four or less channels (estimated from the largest superimposed single-channel current level) were suitable for the present analyses. Each conditional open time of overlapping openings is definitely terminated by the first shut of a channel until an opening occurs. (Note that the sequence of the openings of overlapping events is omitted as the conditional open time is measured from the onset of the postpulse.) Conditional open times of overlapping events were measured on a record until an opening occurred at any of the four threshold levels. Less than 3% of the records had an opening after a shut at level two and no openings occurred at level three. Therefore, the loss of events and thus the calculations resulted in a negligible error. This type of calculation assumes independent opening and closing, and homogeneous population of channels, which conditions are supposed to be fulfilled for all calculations in this paper.

Histograms were fitted by the sum of exponential functions. χ^2 values were calculated for each fit to estimate the number of exponential components of the histograms (Colquhoun & Sigworth, 1983).

Open-time histograms were fitted by the following equation:

$$f(t) = \frac{w_1}{\tau_2 - \tau_1}\left[\exp(-t/\tau_2) - \exp(-t/\tau_1)\right] + \frac{w_2}{\tau_2}\exp(-t/\tau_2) + \frac{w_3}{\tau_3}\exp(-t/\tau_3), \quad (1)$$

where w_i is the area of the ith component, and τ_i its time constant. The first component of this equation consists of the difference of two exponentials which shifts the maximum of the histogram to $t > 0$ (*see* Colquhoun & Hawkes, 1983). Fits of the histograms were obtained by leaving six parameters free, three time constants and three pre-exponential factors.

Results

Different kinetic states of channels can be studied by changing the experimental conditions. In the present work two types of measurements were carried out: a) During repolarization the channel open and conditional open time was studied as a function of the conditioning pulse. b) During a single pulse the time dependence of the open time was investigated. Experiment type a) is equivalent to the macroscopic tail current measurements. Therefore, the conclusions from these experiments are relevant for tail current measurements.

Single-Channel Currents Measured at Repolarizing Voltage Steps

In Fig. 1 single-channel currents are shown recorded during a 2-msec-long pulse V_1 and a postpulse V_2, of different height. In these current records three types of channel openings can be observed: 1) channels which open and close during the pulse V_1, 2) channels which open at V_1 and shut at V_2, and 3) channels which open and shut at V_2. To characterize the length of the channel openings during the postpulse two parameters can be measured: the first is the conditional open time COT, i.e. the time from the onset of V_2 until a channel shuts provided it was open at the end of V_1. The second parameter is the channel open time—marked by OT.

Channels which open at the prepulse and shut at the postpulse can be observed at any postpulse potential if the prepulse potential is in the activation range. Openings of channels at the postpulse may also occur because, first, during a short conditioning pulse a portion of channels neither opens nor inactivates, i.e. stays in the resting state. Secondly, channels being open at the onset of the postpulse may also close to the resting state and can reopen. These openings can be observed if the postpulse potential is positive enough to elicit close-open transitions. In other words, this component contributes to the averaged or macroscopic tail current if the postpulse potential is in the activation range (*see also* Kunze et al., 1985).

The records in Fig. 1 give the impression that the dominating component during the postpulse is due to channels which open during V_1 and shut during V_2. To describe this component conditional open-time histograms were constructed. From the cumulative conditional open-time histograms the probability of finding a channel open, given it was open at the onset of the postpulse, can be calculated. Examples of these probabilities are shown in

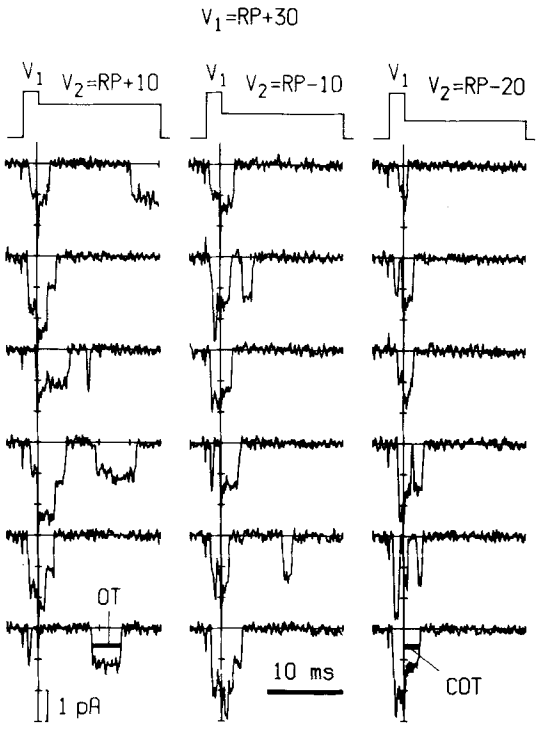

Fig. 1. Single-channel current records measured during a conditioning pulse (V_1) and during postpulses (V_2) in a cell-attached patch. *RP* indicates the resting potential, *OT* the open time and *COT* the conditional open time. Holding potential was *RP*-60 mV, temperature was 8°C

Fig. 2 obtained with a single patch. The scheme in the inset illustrates the principle of calculation. In plot (*a*) the postpulse potential was changed as indicated; for both curves the same conditioning pulse was used. In plot (*b*) the conditioning potential was changed, but the postpulse potential was kept constant. These plots suggest that not only the postpulse but also the conditioning pulse potential influences the time-course of the conditional open-time histograms.

Conditional open-time histograms could be best fitted by the sum of two exponentials at most potentials. Examples of histograms and their fits are shown in Figs. 3(*a*), (*b*) and (*c*). In Fig. 3(*d*) the two time constants of the fits are plotted as functions of the postpulse potential for two conditioning pulse potentials. Here different symbols were used for different patches and the continuous lines were drawn by eye. The slow time constant increased about threefold for a 30-mV increase of the postpulse potential for both conditioning pulses. A tendency to increase might be suspected in the fast time constant for the same potential range.

With decreasing postpulse potential the fast time constant approaches the rise time of the mea-

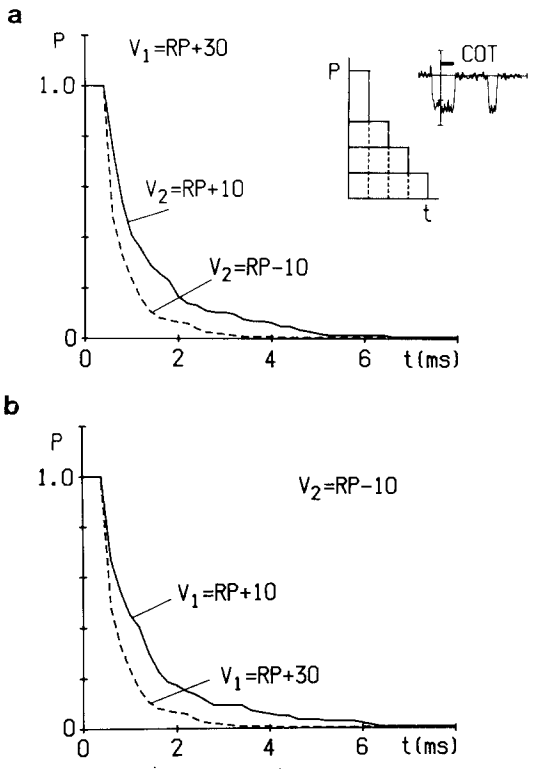

Fig. 2. Dependence of the time-course of the conditional open-channel probability on postpulse potential (*a*) and on prepulse potential (*b*) in a single patch. *P* is the probability of finding a channel open during the postpulse provided it was open at the end of the prepulse. V_1 and V_2 indicate the pre- and postpulse potentials, respectively. The inset illustrates the calculation. *COT* is the conditional open time measured from the onset of the postpulse until the channel shuts. $V_H = RP - 60$ mV, $T = 8$°C. The number of events are for (*a*) 173 and 314 for $RP + 10$ mV and $RP + 30$ mV, respectively; for (*b*) 182 and 314 for $RP + 10$ mV and $RP + 30$ mV, respectively

suring system; therefore, it cannot be calculated exactly (*see* Materials and Methods). These approximate values in Fig. 3(*d*) indicate only an upper limit for the fast time constant.

The stronger conditioning pulse caused a positive shift of the time constants in Fig. 3(*d*). Due to the variable resting potential of the cells (*see* Materials and Methods), values pooled from different patches obtained with different conditioning pulse potentials did not show a significant difference for the fast time constants and for the slow time constants at $V_2 < -10$ mV. In single patches, however, by increasing the conditioning pulse potential, a significant decrease of the time constants at moderate V_2 could always be observed (compare the time constants for Fig. 3(*b*) and (*c*) in Table 1).

A similar voltage dependence and similar numerical values of the slow time constants were also found for the channel open times measured during the postpulse as shown in Fig. 4. In Fig. 4(*a*) mean open times obtained from a single patch are plotted as function of the postpulse potential V_2, for two conditioning pulses. A 30-mV increase in V_2 caused a more than twofold increase in the mean open time for both conditioning pulses. A similar voltage-dependence of the mean channel open time was previously measured with single pulses on outside-out patches (Nagy et al., 1983) and was also reported by Sigworth and Neher (1980), by Vandenberg and Horn (1984) and by Carbone and Lux (1986). The stronger conditioning pulse caused a similar positive shift of the curve as it was observed for the time constants of the conditional open-time histograms (*see* Fig. 3*d*).

Like the conditional open-time histograms the

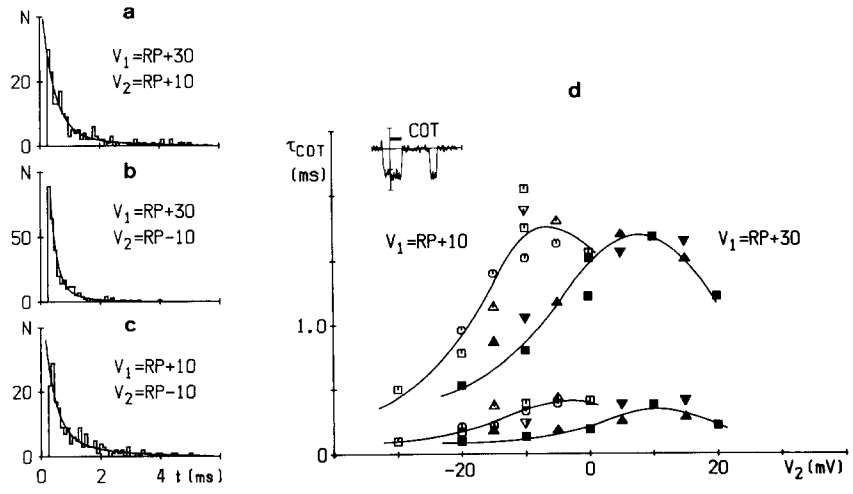

Fig. 3. (*a–c*) Conditional open-time histograms and their fits for the indicated pre- (V_1) and postpulses (V_2) obtained from a single patch. Parameters of the fits are listed in Table 1. (*d*) Dependence of the two time constants of the conditional open-time histograms τ_{COT} on the postpulse potential V_2, for two conditioning pulses V_1. Different symbols were used for different patches; the continuous lines were drawn by eye. Filled and unfilled symbols of identical shape are from the same patch. V_H was between $RP - 50$ and $RP - 70$ mV, $T = 8$°C

unconditional open-time histograms could generally be best fitted by the sum of two exponential functions (Fig. 4*c* and *d*). In some patches the number of events at $V_2 < -10$ mV was so much reduced that no statistical difference between a single or a biexponential fit could be found. The logarithm of the two time constants are plotted as function of V_2 in Fig. 4(*b*). The fast time constant increases with increasing postpulse potential for both conditioning pulses, but the slow time constant shows a moderate decrease. The stronger conditioning pulse caused a definite positive shift of the fast time constant similar to that of the time constants of the conditional open-time histograms, but no change in the slow time constant can be observed.

The similarities between the conditional and unconditional open-time histograms are not surprising, because the conditional open time is actually a residual open time. Therefore, if the channel is memoryless the time constants of the conditional open-time histograms should equal the time constants of the unconditional open-time histograms. [The memoryless gating of channels supposed here is a Markovian assumption (Colquhoun & Hawkes, 1983; French & Horn, 1983; Horn & Vandenberg, 1984), which is not fulfilled for the other parts of the results; *see* Discussion.]

For comparison, Fig. 5 shows the time constants of the conditional open-time histograms and the fast time constants of the open-time histograms in the same plot as function of the postpulse potential. These values are obtained from a single patch. The slow time constants of the open-time histograms are out of scale in these plots. In Fig. 5(*b*) the conditioning pulse potential was 20 mV more posi-

Table 1. Parameters for Figs. 3 and 4[a]

Fig.	τ_1	τ_2	w_1	w_2	$\chi^2(df)$	P	ΣN
3(*a*)	0.40	1.68	0.75	0.25	14.2(15)	0.51	173
3(*b*)	0.20	0.78	0.84	0.16	11.4(10)	0.33	314
3(*c*)	0.39	1.77	0.55	0.45	15.1(14)	0.37	182
4(*c*)	1.66	5.8	0.91	0.09	9.6(19)	0.96	155
4(*d*)	0.81	5.1	0.82	0.18	12.9(16)	0.68	117

[a] Time constants τ_i, weighting factors w_i, chi-square values χ^2, degrees of freedom df, P values and the sum of events ΣN are listed.

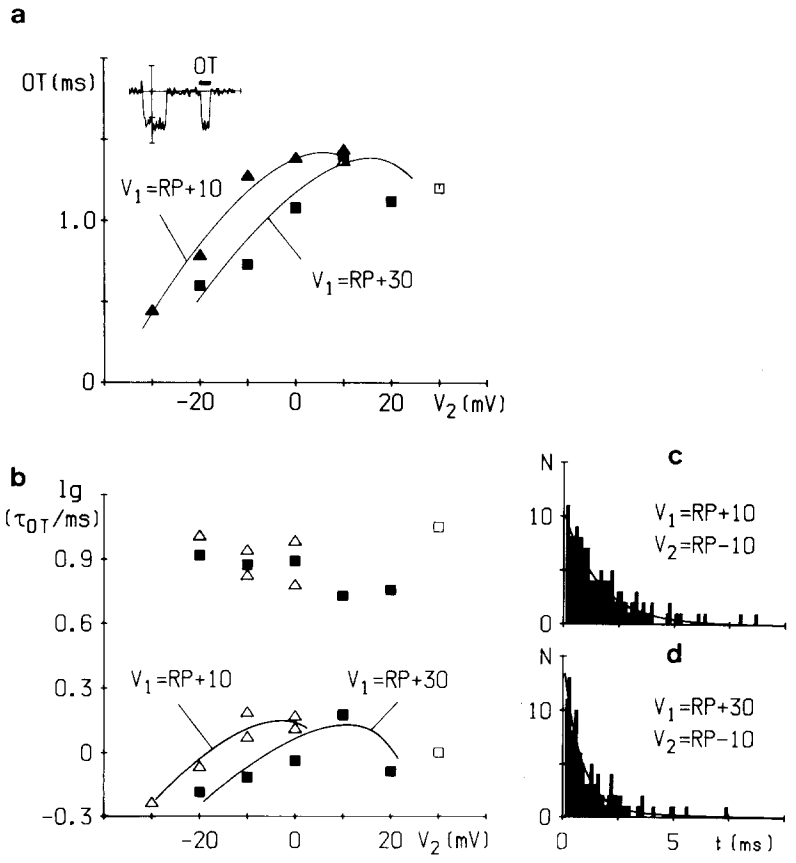

Fig. 4. Mean values of the channel open time (*a*) and the logarithm of the time constants of the open-time histograms (*b*) as function of the postpulse potential V_2, for two conditioning pulse potentials V_1. (*c*) and (*d*) are examples of open-time histograms and their fits resulting in parameters as listed in Table 1. All plots are from a single patch. Two identical symbols in (*b*) at the same potential refer to two series of records measured at different times during the long experiment. Open squares in (*a*) and (*b*) indicate values measured without conditioning pulse. $V_H = RP - 70$ mV, $T = 8$°C

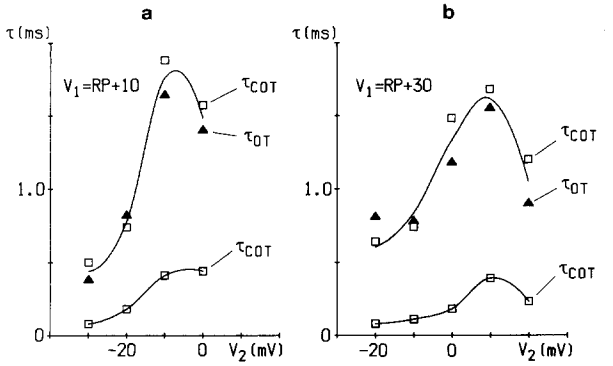

Fig. 5. Comparison of the time constants of the conditional open-time histograms τ_{COT} and the fast time constant of the unconditional open-time histogram τ_{OT} for two conditioning pulses V_1. Plots are from a single patch. $V_H = RP - 60$ mV, $T = 8$°C

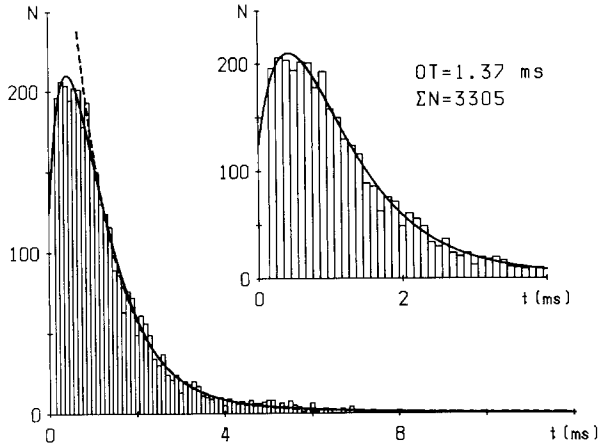

Fig. 6. Open-time histogram obtained from a single pulse experiment with a single patch. The patch was depolarized by a 40-msec-long pulse to the resting potential. $V_H = RP - 80$ mV, $T = 8$°C. The dashed line is the sum of two exponentials fitted to the histogram in the range of 0.9 to 12 msec resulting in the time constants of 0.92 and 5.70 msec. In this range the chi-square value (degrees of freedom) is 27.6 (39), $P = 0.91$. The continuous line shows the function given by Eq. (1). Parameters obtained from the fit are listed in Table 2. In the inset the 0- to 4-msec range of the histogram and the fit are replotted on expanded time scale. OT is the mean open time, ΣN is the number of events

tive than in Fig. 5(*a*). These plots emphasize the close similarity between the slow time constants of the conditional open-time and the fast time constants of the unconditional open-time histograms.

Differences between the conditional and unconditional open-time histograms also appear. a) The conditional open-time histograms have no time constants >2 msec, which would be similar to that of the slow time constants (>4 msec) of the open-time histograms. Such slow time constants were never observed for conditional open-time histograms in the eight experiments made with different pre- and postpulse potentials. b) The open-time histograms seems to have no time constants <0.5 msec, which would be similar to the fast time constants of the conditional open-time histograms. However, this conclusion is only preliminary (*see below*).

The fast time constants of the conditional open-time histograms are difficult to measure correctly (*see* Materials and Methods) and might be biased by the activation time course at the conditioning pulse in the sense that channels which open first close first. If the fast time constant reflects a molecular process, one should also find a similar time constant in the open-time histograms. A time constant <0.5 msec is difficult to measure and when present it is difficult to separate from other time constants of a histogram. Since the number of openings during the postpulse was small (*see* Fig. 1), it may be supposed that it was impossible to collect enough data to separate a fast component in the open-time histograms. Therefore, experiments with single pulses have been made to collect sufficient data for statistical analyses.

Open Time of Channels Measured with Single Pulses

In these experiments moderate pulse potentials were chosen for two reasons: a) A straightforward analysis of the open time requires nonoverlapping openings (Horn & Standen, 1983). As patches contained two to six channels, the occurrence of overlapping events could be reduced by choosing moderate potentials. Less than 11% of openings overlapped in the present experiment. Records having overlapping openings were omitted from the calculations. b) A further aim was to study the time dependence of the channel open time. At large pulse potentials openings would tend to be shifted toward the onset of the pulse and so the time interval to be examined would have been compressed.

Figure 6 shows an open-time histogram obtained from a single patch depolarized 4000 times by a single pulse to the resting potential. The decaying phase of the histogram (between 0.9 and 12 msec) could be fitted by the sum of two exponentials as shown by the dashed line. The obtained two time constants support the idea suggested earlier (Nagy et al., 1983) that sodium channels in neuroblastoma cells may have two open states. However, fitting only the decaying phase of the histogram, events

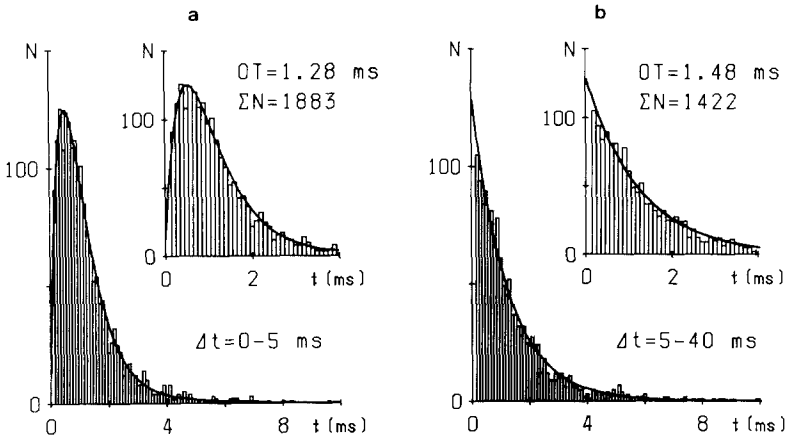

Fig. 7. Open-time histograms from the early and late phase of depolarization. The histogram is constructed from openings appearing during the time interval Δt = 0 to 5 msec (*a*) and Δt = 5 to 40 msec (*b*). Plots are from the same experiment as Fig. 6. Parameters of the fits (continuous lines) are listed in Table 2. In the insets the 0- to 4-msec ranges of the histograms are replotted on enlarged time scale. Mean open time (*OT*) and the number of events (ΣN) are also shown

having open times shorter than 0.9 msec are omitted. This omitted portion of the histogram is 41% of all events, which may not be disregarded. Consequently, an exponential function with two time constants is an unsatisfactory fit for the whole histogram.

The large deficiency of the measured events compared to the biexponential function at short open times in Fig. 6 cannot be explained by an experimental or measuring artifact due to two reasons: a) It was discussed in Materials and Methods that 0.2 msec or longer open times can be measured exactly. b) It will be shown that an open-time histogram constructed in a later phase of the depolarization does not have any deficiency at short open times (*see* e.g. Fig. 7*b*). Therefore, it may be stated that the histogram in Fig. 6 does not have a monotonically decaying phase, but it has a maximum at $t > 0$. The maximum of the histogram is at about 0.4 msec, which is more than four times larger than the dead time of the measuring system.

Histograms having a maximum at $t > 0$ can be fitted by the difference of two exponential terms (*see* Colquhoun & Hawkes 1983), suggesting two open states (O_1 and O_2 in the scheme below), which are in sequence. Tentatively, the pathways of channels can be described by the following scheme:

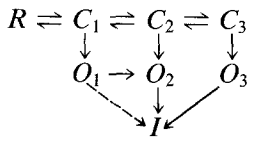

Here R, C_i, O_i and I represent the resting, the ith closed, the ith open and the inactivated state, respectively. The best fit of the histogram in Fig. 6 could be obtained by Eq. (1) given in Materials and Methods. This function has three terms. The first term contains the difference of two exponentials, resulting in the maximum of the histogram, as mentioned. The two time constants of this term are 0.51 and 0.65 msec (*see* Table 2), which are the life-times of the two open states sequentially coupled. This term has the largest weight, 0.66 (*see* Table 2). The second term having a weight of 0.20 has the same time constant (0.65 msec) as the slower component of the first term. The third term with a weight of 0.14 and the time constant of 3.59 msec is the slowest component. The second term suggests that this open state (O_2 in the above scheme) may also appear alone, not only in sequence with the shortest (O_1) open state. The fastest time constant (τ_1 = 0.51 msec) is in the same range as the fast time constants of the conditional open-time histograms shown in Figs. 3 and 5. Therefore, it may be supposed that the fast time constants of the conditional open-time histograms indicate a real, molecular process.

It was reported that channels which open late during the depolarization tend to stay open longer (Sigworth, 1981; Nagy et al., 1983). The time dependence of the channel open time was studied in the present experiments, too. Open-time histograms constructed from openings before and after 5.0 msec are shown in Fig. 7(*a*) and (*b*), respectively. To emphasize the difference between the two plots the short open-time ranges of the histograms are plotted in the insets on expanded time scales. Clearly, the histogram in Fig. 7(*b*) has a monotonically decaying phase, whereas that in Fig. 7(*a*) has a maximum around 0.5 msec. The histograms were fitted by Eq. (1). The parameters of the fits are listed in Table 2. In the last phase of depolarization (Fig. 7*b*) both time constants are larger than those of the corresponding components of the early phase. (Compare also the mean open times (OT) given in Fig. 7*a* and *b*.) The first term of Eq. (1) (i.e. the

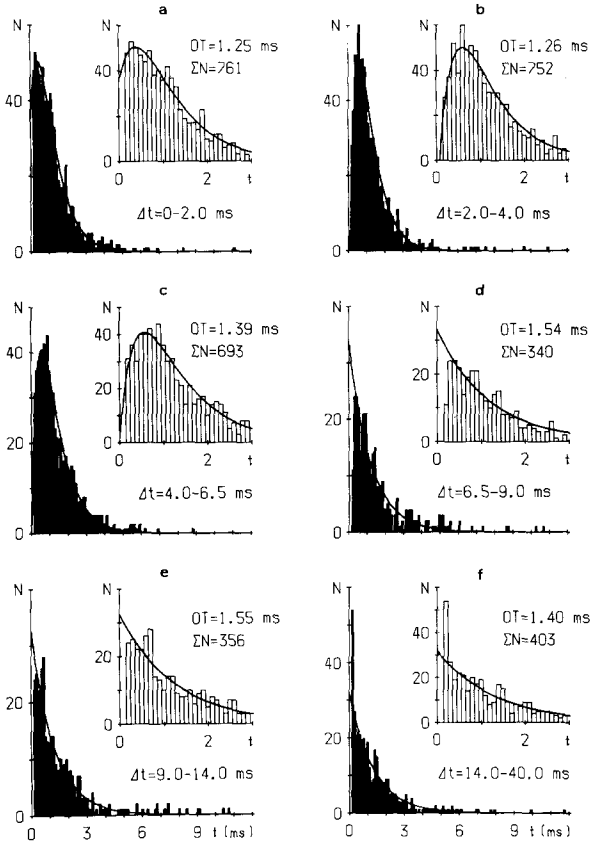

Fig. 8. Open-time histograms and their fits (continuous lines) for the indicated time intervals (Δt) of the depolarization. Histograms are from the same experiment as Figs. 6 and 7. Parameters of the fits are listed in Table 2. Mean open times (OT) and the number of events (ΣN) are indicated

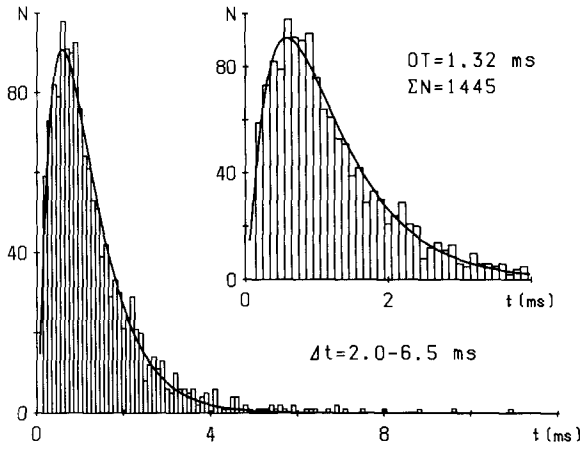

Fig. 9. The sum of the histograms shown in Fig. 8(*b*) and (*c*). The histogram could be best fitted by the difference of two exponentials (continuous line) with time constants of 0.34 and 0.83 msec (*see also* Table 2). Δt indicates the time interval, OT the mean open time and ΣN the number of events. The inset shows the short open time range of the histogram and fit on expanded time scale

difference of two exponentials) has the largest weight for Fig. 7(*a*) ($w_1 = 0.85$) but is zero for Fig. 7(*b*). Consequently, in the early phase of depolarization the two coupled open states (O_1 and O_2) are dominating, but in the late phase these states or the irreversible coupling cannot be observed. The fact that the open-time histogram in Fig. 7(*b*) has a monotonic decaying phase excludes the possibility that the maximum at $t > 0$ in Figs. 6 and 7(*a*) is due to an experimental or calculating artifact.

The time dependence of the open time was further studied by dividing the depolarization into six intervals, in which open-time histograms have been constructed. These histograms are shown in Fig. 8. In the insets, for better comparison, the 0 to 3 msec time ranges of the histograms are displayed on expanded time scale. Fits of the histograms by Eq. (1) resulted in parameters listed in Table 2. In the time interval 0 to 2.0 msec the first and the second components are present ($w_1 = 0.63$, $w_2 = 0.37$, *see* Table 2). Between 2.0 and 4.0 msec the first component alone results in a good fit and between 4.0 and 6.5 msec the second component makes only a minor contribution to the fit ($w_2 = 0.04$). After 6.5 msec the first component disappears. With increasing time the time constant τ_2 is gradually increasing from 0.80 to 1.31 msec (except the interval of 2.0 to 4.0 msec). Noteworthy, the first bin of the histogram in Fig. 8(*d*) is significantly smaller than could be expected from the fit obtained by the sum of two exponentials. Contrary to this, the first bin of the histogram in Fig. 8(*f*) is significantly larger than the exponential fit. However, the lack of sufficient data made the further analysis of this question impossible. The plots in Fig. 8 and the parameters listed in Table 2 clearly demonstrate a gradual change of the open-time histograms with increasing time.

In the time intervals 2.0 to 4.0 msec and 4.0 to 6.5 msec the presence of the coupled open states is most evident. Therefore the sum of the histograms of Fig. 8(*b*) and (*c*) is replotted in Fig. 9. This histogram has a maximum at about 0.6 msec and could be best fitted by the difference of two exponentials with the time constants 0.34 and 0.83 msec (*see* Table 2). Outside the interval of 2.0 to 6.5 msec either the same open states may appear independently or other open states may occur.

It was reported that during subsequent depolarizations records with and without openings are grouped in runs (Horn et al., 1984; Kiss & Nagy, 1985). The positive value of the variable Z indicates a tendency for nonrandom appearance of runs (*see* Horn et al., 1984; Colquhoun & Sakmann, 1985). Z was 2.24 for the experiment, from which the open-time histograms in Figs. 6, 7, 8 and 9 are

Table 2. Parameters for Figs. 6, 7, 8 and 9[a]

Fig.	Δt (msec)	w_1	w_2	w_3	τ_1 (msec)	τ_2 (msec)	τ_3 (msec)	χ^2 (df)	P
6	0–40	0.66	0.20	0.14	0.51	0.65	3.59	30.7 (46)	0.96
7(*a*)	0–5	0.85	0.08	0.07	0.44	0.60	2.18	20.9 (31)	0.91
7(*b*)	5–40	0	0.84	0.16	—	1.15	3.63	22.6 (35)	0.95
8(*a*)	0–2.0	0.63	0.37	0	0.48	0.80	—	15.3 (23)	0.88
8(*b*)	2.0–4.0	1.00	0	0	0.40	0.67	—	11.7 (21)	0.95
8(*c*)	4.0–6.5	0.96	0.04	0	0.37	0.92	—	15.8 (23)	0.86
8(*d*)	6.5–9.0	0	0.97	0.03	—	1.09	5.48	9.4 (14)	0.80[b]
8(*e*)	9.0–14.0	0	0.92	0.08	—	1.20	7.06	15.5 (20)	0.75
8(*f*)	14.0–40.0	0	1.00	0	—	1.31	—	12.3 (12)	0.42[c]
9	2.0–6.5	1.00	0	0	0.34	0.83	—	23.2 (33)	0.90

[a] w_i and τ_i are the weighting factors (the area of the ith component) and the time constants of the components, respectively. Δt is the time interval in which the open times were measured. Chi-square values (χ^2), degrees of freedom (df) and the corresponding P values are also listed.
[b] and [c]: The fits and the chi-square values were obtained after omitting the first bin of the histograms. Including the first bin the values are: [b] $\chi^2(df) = 19.7\ (15)$, $P = 0.18$; [c] $\chi^2(df) = 39.0\ (13)$, $P = 2 \times 10^{-4}$.

demonstrated, indicating significant clustering of records with openings. However, open-time histograms constructed from openings which appeared on the first, second and third record of a run were only slightly different.

Discussion

The main goal of this work is to provide evidence for multiple open states of sodium channels in neuroblastoma cells. Previously, open-time histograms fitted by the sum of two exponential functions gave an indication for two open states (Nagy et al., 1983). However, if histograms are constructed from multichannel patches heterogeneous kinetics of channels or different population of channels cannot be excluded with certainty. The present finding that the open-time histogram in the 2.0- to 6.5-msec time range is best fitted by the difference of two exponentials gives convincing evidence for the presence of two open states of channels. This fit provides further information about the relation of the states. Namely, these open states (O_1 and O_2 in the scheme on page 257) must be connected through an irreversible pathway. Another mechanism by which an open-time histogram with a maximum at $t > 0$ could be explained is not known (*see* Colquhoun & Hawkes, 1983). The first finding of an open-time distribution having a maximum at $t > 0$ was reported by Gration et al. (1982). They measured the open times of glutamate channels in extrajunctional membrane of locust muscle and suggested an irreversible two-step process for channel closing.

The experimental results show similarities between the time constants of the conditional and the unconditional open-time histograms. This suggests that both types of calculations give information about the same molecular process, i.e. about the channel closing. Therefore the multiexponential decay of the conditional and the unconditional open-time histograms (presented here) and of the tail currents (described by Goldman and Hahin, 1978, and Schauf et al., 1977) may indicate multiple open states of sodium channels. Similarity between the conditional and unconditional open times can be observed since certain open states occur in both histograms. Differences between the conditional and unconditional open-time histograms (*see* page 256) could also be explained by the presence of multiple open states. Concluding from the observed time dependence of the open-time histogram, different open states may occur at the end of the conditional pulse than later during the postpulse.

The experiments show that the time constants

of the conditional and unconditional open-time histograms depend on the prepulse potential. This observation indicates contradiction to the Markovian assumption of the memoryless gating of channels. Initial condition-induced changes have been reported for the time constant of the macroscopic inactivation by Chandler and Meves (1970) and for the time course of the tail currents by Goldman and Hahin (1978) and by Sigworth (1981). The change of the time constants with the initial conditions can be explained either by the aggregation model of Baumann (1981, 1983), or by assuming that the calculated time constants are the mean of two or more time constants, whose weight changes with the initial conditions (*see* Goldman & Hahin, 1978). It was shown that having sufficient data a fast component could be observed in the unconditional open-time histogram. Therefore it can be supposed that the calculated time constants of the conditional and unconditional open-time histograms obtained from the double-pulse experiments are the mean values of two or more time constants, which could not be separated. This conclusion also supports the idea that the sodium channels in neuroblastoma cells may have several open states.

The experiments also provide new evidence for the time dependence of the channel open time. This phenomenon has first been reported by Sigworth (1981). He showed that in the node of Ranvier channels which open late during a depolarization stay open longer. Similar conclusions were reached for sodium channels in neuroblastoma cells (Nagy et al., 1983). The present results support the previous conclusions. Furthermore, they suggest that the relation between the open states is rather complicated (*see* scheme on page 257). Open-time histograms constructed for different time intervals of the depolarization indicated that an irreversible pathway between the open states O_1 and O_2 is most probable between 2.0 and 6.5 msec. Before and after this interval either the two coupled open states appear less frequently and other open states occur, or the coupled states open independently. It was shown that the time constant τ_2 (which is always existent) increases gradually with increasing time. τ_2 is the slower time constant of the coupled states before 6.5 msec of the depolarization and it represents an independent (single) open state (O_2) after 6.5 msec. Therefore, it might be supposed that the connection between the coupled states is changed during the depolarization. (This idea might also be supported by Fig. 8(*f*), in which the first bin of the histogram is significantly larger than the fit suggesting an additional fast component.)

The gradual increase of the time constant τ_2 with increasing time could be explained (similarly to the initial condition-induced changes of time constants) by supposing that it is the mean of two or more time constants which could not be separated.

The usual models developed for the sodium channels assume a) a time homogeneous and b) an irreducible Markov process. (These conditions mean that the transition rates are time independent and that all states can be reached from any other states; French & Horn, 1983.) According to the present results both assumptions appear to be violated: a) the open-time histograms were time dependent indicating time-dependent transition probabilities; b) an irreversible pathway was found between two open states. Previous indications against the Markovian assumptions are summarized by French and Horn (1983). All these findings suggest that for sodium channels in some preparations a more complex model has to be developed.

An alternative explanation for the observed time dependence of the channel open time would be the presence of at least two populations of channels. One population should have two open states coupled irreversibly, the other population (or populations) should form the sum of two exponentials of the open-time histograms in the last phase of the depolarization. This alternative possibility cannot be excluded with certainty. However, it was shown that both native and sea anemone toxin-modified channels have discrete, different single-channel current levels (Nagy & Bagany, 1986; Nagy, 1987). This also suggests that channels may have different open conformations.

The multiexponential open-time histograms with a maximum at $t > 0$ reported in the present paper differ from the open-time histograms published by Fukushima (1981), Quandt and Narahashi (1982), Aldrich et al (1983), Horn and Vandenberg (1984) and Carbone and Lux (1986). Their open-time histograms can be fitted by a single exponential, suggesting a single open state of sodium channels. Possible explanations for the discrepancy are as follows: a) A general explanation. To observe multiexponential open-time histograms a lot of data must be collected under the same experimental conditions. For instance, Figs. 6, 7, 8 and 9 were obtained from a single patch depolarized 4000 times. Having insufficient data significant deviations from a single exponential, especially in the short open-time range can be missed. The time dependence of the time constants of the open-time histograms can only be studied at moderate depolarizations, where the openings appear on an expanded time scale. However, then the number of openings is small reducing the significance level of statistical tests. b) The limited frequency range of the method does not make it possible to observe a fine structure at higher

temperature. For instance, calculating with a Q_{10} ~2.2 (unpublished value obtained for the time constants of the open-time histograms) faster time constants than 1.0 msec at 8°C (which would be 0.45 msec at 18°C) cannot be separated and measured correctly at room temperature. The high temperature might explain why Aldrich et al. (1983) did not report a maximum for the open-time histograms measured at 16°C or higher temperatures. c) Differences in preparations. Fukushima (1981) used tunicate egg cells, Horn and Vandenberg (1984) GH_3 cells, Carbone and Lux (1986) dorsal root ganglion neurons. The multiexponential open-time histograms presented here may indicate differences between sodium channels in different preparations. d) Differences between cell-attached patches (as used in the present work) and excised patches (as used by Quandt and Narahashi, 1982).

The multiple open states of sodium channels and the time-dependent time constant of the open-time histograms indicate that simplified kinetic models can give only an overall description, but on a molecular level the function of channels can be much more complex, at least in some preparations.

I thank Professor H. Meves for support, helpful discussions and comments on the manuscript, Dr. T. D. Plant for comments on the manuscript. Thanks to Dr. D. Hof for writing computer programs and Mrs. R. Stolz for typing the manuscript. This work was supported by the Deutsche Forschungsgemeinschaft (SFB 38 and 246).

References

Aldrich, R.W., Corey, D.P., Stevens, C.F. 1983. A reinterpretation of mammalian sodium channel gating based on single channel recording. *Nature (London)* **306**:436–441

Armstrong, C.M., Bezanilla, F. 1977. Inactivation of sodium channel. II. Gating current experiments. *J. Gen. Physiol.* **70**:567–590

Armstrong, C.M., Gilly, W.F. 1979. Fast and slow steps in the activation of sodium channels. *J. Gen. Physiol.* **74**:691–711

Baumann, G. 1981. Novel kinetics in the sodium conductance system predicted by the aggregation model of channel gating. *Biophys. J.* **35**:699–705

Baumann, G. 1983. Stochastic modeling of the aggregation-gating site. *In:* Structure and Function in Excitable Cells. D.C. Chang, I. Tasaki, W.J. Adelman, and H.R. Leuchtag, editors. pp. 255–271. Plenum, New York–London

Blatz, A.L., Magleby, K.L. 1986. Correcting single channel data for missed events. *Biophys. J.* **49**:967–980

Cachelin, A.B., DePeyer, J.E., Kokubun, S., Reuter, H. 1983. Sodium channels in cultured cardiac cells. *J. Physiol. (London)* **340**:389–401

Carbone, E., Lux, H.D. 1986. Na channels in cultured chick dorsal root ganglion neurons. *Eur. Biophys. J.* **13**:259–271

Chandler, W.K., Meves, H. 1970. Evidence for two types of sodium conductance in axons perfused with sodium fluoride solution. *J. Physiol. (London)* **211**:653–678

Colquhoun, D., Hawkes, A.G. 1983. The principles of the stochastic interpretation of ion-channel mechanisms. *In:* Single Channel Recording. B. Sakmann and E. Neher, editors. pp. 135–175. Plenum, New York

Colquhoun, D., Sakmann, B. 1985. Fast events in single-channel currents activated by acetylcholine and its analogues at the frog muscle endplate. *J. Physiol. (London)* **369**:501–557

Colquhoun, D., Sigworth, F.J. 1983. Fitting and statistical analysis of single-channel records. *In:* Single Channel Recording. B. Sakmann and E. Neher, editors. pp. 191–263. Plenum, New York

Frankenhaeuser, B., Hodgkin, A.L. 1957. The action of calcium on the electrical properties of squid axons. *J. Physiol. (London)* **137**:218–244

French, R.J., Horn, R. 1983. Sodium channel gating: Models, mimics and modifiers. *Annu. Rev. Biophys. Bioeng.* **12**:319–356

Fukushima, Y. 1981. Identification and kinetic properties of the current through a single Na^+ channel. *Proc. Natl. Acad. Sci. USA* **78**:1274–1277

Gilly, W.F., Armstrong, C.M. 1984. Threshold channels—a novel type of sodium channel in squid giant axon. *Nature (London)* **309**:448–450

Goldman, L., Hahin, R. 1978. Initial conditions and the kinetics of the sodium conductance in Myxicola giant axons. *J. Gen. Physiol.* **72**:879–898

Gration, K.A.F., Lambert, J.J., Ramsey, R.L., Rand, R.P., Usherwood, P.N.R. 1982. Closure of membrane channels gated by glutamate receptors may be a two-step process. *Nature (London)* **295**:599–601

Hamill, O.P., Marty, A., Neher, E., Sakmann, B., Sigworth, F.J. 1981. Improved patch clamp techniques for high-resolution current recording from cells and cell-free membrane patches. *Pfluegers Arch. Eur. J. Physiol.* **391**:85–100

Hof, D. 1986. A pulse generating and data recording system based on the microcomputer PDP 11/23. *Comput. Method. Program. Biomed.* **23**:309–315

Horn, R., Standen, N.B. 1983. Counting kinetic states: The single channel approach. *In:* The Physiology of Excitable Cells. A. Grinnell and W. Moody, editors. pp. 181–189. A.R. Liss, New York

Horn, R., Vandenberg, C.A. 1984. Statistical properties of single sodium channels. *J. Gen. Physiol.* **83**:505–534

Horn, R., Vandenberg, C.A., Lange, K. 1984. Statistical analyses of single sodium channels. Effects of N-bromoacetamide. *Biophys. J.* **45**:323–335

Kiss, T., Nagy, K. 1985. Interaction between sodium channels in mouse neuroblastoma cells. *Eur. Biophys. J.* **12**:13–18

Kostyuk, P.G., Veselovsky, N.S., Tsyndrenko, A.Y. 1981. Ionic currents in the somatic membrane of rat dorsal root ganglion neurons. I. Sodium currents. *Neuroscience* **6**:2423–2430

Kunze, P.L., Lacerda, A.E., Wilson, D.L., Brown, A.M. 1985. Cardiac Na currents and the inactivating, reopening, and waiting properties of single cardiac Na channels. *J. Gen. Physiol.* **86**:691–719

Moolenaar, W.H., Spector, I. 1978. Ionic currents in cultured mouse neuroblastoma cells under voltage-clamp conditions. *J. Physiol. (London)* **278**:265–286

Nagy, K. 1987. Subconductance states of single sodium channels modified by chloramine-T and sea anemone toxin in neuroblastoma cells. *Eur. Biophys. J. (in press)*

Nagy, K., Bagany, M. 1986. Multiple discrete single sodium channel current levels in neuroblastoma cells. *Proc. Int. Union Physiol. Sci.* **Vol. XVI**, p. 441

Nagy, K., Kiss, T., Hof, D. 1983. Single Na channels in mouse neuroblastoma cell membrane. Indications for two open states. *Pfluegers Arch. Eur. J. Physiol.* **399:**302–308

Neumcke, B., Stämpfli, R. 1983. Alteration of the conductance of Na^+ channels in the nodal membrane of frog nerve by holding potential and tetrodotoxin. *Biochim. Biophys. Acta* **727:**177–184

Patlak, J., Horn, R. 1982. Effect of N-bromoacetamide on single sodium channel currents in excised membrane patches. *J. Gen. Physiol.* **79:**333–351

Patlak, J.B., Ortiz, M. 1986. Two modes of gating during late Na^+ channel current in frog sartorius muscle. *J. Gen. Physiol.* **87:**305–326

Patlak, J.B., Ortiz, M., Horn, R. 1986. Open time hetereogeneity during bursting of sodium channels in frog skeletal muscle. *Biophys. J.* **49:**773–777

Quandt, F.N., Narahashi, T. 1982. Modification of single Na^+ channels by batrachotoxin. *Proc. Natl. Acad. Sci. USA* **79:**6732–6736

Roux, B., Sauvé, R. 1985. A general solution to the time interval omission problem applied to single channel analyses. *Biophys. J.* **48:**149–158

Schauf, C.L., Bullock, J.O., Pencek, T.L. 1977. Characteristics of sodium tail currents in Myxicola axons. Comparison with membrane asymmetry currents. *Biophys. J.* **19:**7–28

Sigworth, F.J. 1981. Covariance of nonstationary sodium current fluctuations at the node of Ranvier. *Biophys. J.* **34:**111–133

Sigworth, F., Neher, E. 1980. Single Na^+ channel currents observed in cultured rat muscle cells. *Nature (London)* **287:**447–449

Sine, S.M., Steinbach, J.H. 1986. Activation of acetylcholine receptors on clonal mammalian BC3H-1 cells by low concentrations of agonist. *J. Physiol. (London)* **373:**129–162

Vandenberg, C.A., Horn, R. 1984. Inactivation viewed through single sodium channels. *J. Gen. Physiol.* **84:**535–564

Weiss, R.E., Horn, R. 1986. Functional differences between two classes of sodium channels in developing rat skeletal muscle. *Science (London)* **233:**361–364

Received 26 September 1986; revised 27 January 1987